

Project no.:

608608

Project acronym:

MiReCOL

Project title:

Mitigation and remediation of leakage from geological storage

Collaborative Project

Start date of project: 2014-03-01

Duration: 3 years

D9.1

CO₂ reactive suspensions

Revision: 1

Organisation name of lead contractor for this deliverable:

IFPEN

Project co-funded by the European Commission within the Seventh Framework Programme		
Dissemination Level		
PU	Public	X
PP	Restricted to other programme participants (including the Commission Services)	
RE	Restricted to a group specified by the consortium (including the Commission Services)	
CO	Confidential , only for members of the consortium (including the Commission Services)	

Deliverable number:	D9.1
Deliverable name:	CO ₂ reactive suspensions
Work package:	WP 9.1 Novel materials and technologies for remediation of well leakage
Lead contractor:	IFPEN

Status of deliverable		
Action	By	Date
Submitted (Author(s))	Marc Fleury	30/06/2016
Verified (WP-leader)	Marc Fleury	
Approved (SP-leader)	Robert Drysdale	06/07/2016

Author(s)		
Name	Organisation	E-mail
Marc Fleury	IFPEN	marc.fleury@ifpen.fr
Olivier Sissmann	IFPEN	olivier.sissmann@ifpen.fr
Etienne Brosse	IFPEN	etienne.brosse@ifpen.fr
Michel Chardin	IFPEN	michel.chardin@ifpen.fr

Public abstract
<p>This report is part of the research project MiReCOL (Mitigation and Remediation of CO₂ leakage) funded by the EU FP7 programme. Research activities aim at developing a handbook of corrective measures that can be considered in the event of undesired migration of CO₂ in the deep subsurface reservoirs. MiReCOL results support CO₂ storage project operators in assessing the value of specific corrective measures if the CO₂ in the storage reservoir does not behave as expected. MiReCOL focuses on corrective measures that can be taken while the CO₂ is in the deep subsurface. The general scenarios considered in MiReCOL are 1) loss of conformance in the reservoir (undesired migration of CO₂ within the reservoir), 2) natural barrier breach (CO₂ migration through faults or fractures), and 3) well barrier breach (CO₂ migration along the well bore).</p> <p>This element of MiReCol aims at studying a method for treating the surroundings of a well using a reactive suspension. Ideally, the injected solution should react with the CO₂ present in the formation. Because the amount of CO₂ may be insufficient or even absent, we extended the study to include reactions with an activator (acid). The objective is typically to inject the product around the well, up to a radius of 1 m in order to create a permeability barrier.</p> <p>The study comprises laboratory tests using sandstones representative of geological formations suitable for CO₂ storage but also specific samples from the Becej field in collaboration with NIS (Naftna industrija Srbije, Serbia). Indeed, in a second phase of the project, field tests are expected to be implemented to demonstrate the efficiency of the proposed method. Hence, the design of the process is intimately linked to the field constraint, i.e., sufficient time is needed between the preparation at the surface and the injection of the solution into the formation downhole.</p> <p>Silica-alkaline solutions are aqueous solutions containing high concentrations of SiO₂ and A₂O, where the alkaline element A is generally sodium (Na) or potassium (K). Commercial stable solutions exist with high molar ratio SiO₂/A₂O, spanning from 1.6 up to 3.9 with pH values above 11.5. When the pH is lowered either in contact with CO₂ or using an acid, silica</p>

precipitates to form particles. Below a pH of approximately 9 according to the solubility curve, the particles formed are stable and no back-dissolution is possible unless the pH is increased again. Hence, one expects a long-term stable chemical stability.

An experimental investigation of the precipitation of commercial solutions using a weak acid to lower the pH has been performed. Preliminary results using CO₂ indicate that the reaction kinetics are too fast and difficult to control, and the plugging too strong to allow practical field implementation. Various concentrations of acetic acid added to the commercial silica-based solution were tested, and the bulk gelation times measured before the mixture becomes too viscous for injection. The impact of temperature was determined by performing experiments at 20, 40 and 60°C, with gelation times estimated between a few minutes up to 4 days. To follow the kinetics, several complementary techniques were used: rheological visco-elastic properties to observe the gelling onset, NMR relaxation time measurements to follow the gradual increase of water interactions within the gel.

The ability of the precipitates to plug a porous media was tested on analog sandstone samples representative of CO₂ storage formations, as well as a sample from the Becej field (Serbia). With a viscosity close to that of water and no particles present in the liquid, injection of such products is possible in almost any permeable media. Using an optimum mixture tuned as described above, the solution is simply injected through the porous media and then kept at constant temperature (e.g. 40 °C) for precipitation. After a few days, a breakthrough experiment is performed by increasing gradually the differential pressure across the sample. The results obtained so far indicate a very large strength of the order of 600 bar/m.

TABLE OF CONTENTS

1	GENERAL PRINCIPLES	2
2	LITERATURE REVIEW	5
2.1	Sodium silicate solution as a flow diversion control in the oil industry	6
2.2	Sodium silicate solution as a consolidation material	11
2.3	Chemical characterization and speciation modelling of silico-alkaline solutions.....	12
2.4	Physical properties of sodium silicate alkaline solution.....	18
3	EXPERIMENTAL RESULTS	20
3.1	Solution characterization	20
3.2	Batch experiments: precipitation using CO ₂	22
3.3	Experiments in porous media with CO ₂	26
3.4	Precipitation using CO ₂ : conclusions	27
3.5	Batch experiments: precipitation using acetic acid	27
3.6	Measurements of gelling times.....	29
3.7	Effect of temperature and acid concentration.....	30
3.8	Experiments in porous media with acetic acid	32
4	SUMMARY AND CONCLUSION	34
5	ACKNOWLEDGEMENTS	35
6	REFERENCES	36
7	APPENDIX: BETOL K28 T SOLUTION	38

1 GENERAL PRINCIPLES

A large number of methods can be used to treat the surrounding of a well (Manceau *et al.*, 2014). The objective here is to inject a solution around the well in a selected depth interval (a few meters) in order to plug the formation, i.e., reduce porosity and permeability ideally down to zero. Hence, CO₂ flow at this depth interval cannot occur. Schematically, the envisaged process is such that the porosity should be filled with a solid, and this solid is the result of the precipitation of some components of the injected solution.

Some key requirements are:

- long term stability (one year or more),
- injectivity: the solution should not be too viscous, nor contain too large particles,
- reactivity: the solution should not react outside the geologic formation, and especially in the well during injection; i.e., the reaction should not be too fast for practical reasons.

Beside other possibilities such as cement or resins, a first initial choice was to select a process among two main categories: the precipitation of carbonate or silicate alkaline solutions. For example, using a lime solution:



or using a silicate solution (water glass):



In the latter, amorphous silica is formed when the pH is low enough, for example at the plateau value of solubility (other solids are formed at intermediate pH values). The difference can be viewed in terms of the solubility of calcium and silica in alkaline solutions (Figure 1). As a function of pH, the solubility of silica is much higher and potentially, the amount of solid that can be formed is much higher. Another strong argument in favor of silicates is related to their stability: indeed, below a pH of about 9 (Figure 1), no dissolution occurs and a plateau of solubility is present. This is not the case for carbonates for which the solubility is still evolving around a neutral pH and below. In a geological formation containing CO₂, the pH could still change as a function of the brine-rock-CO₂ equilibrium but there is no known process able to bring pH values back to 9 and above. Hence, the generated solids plugging the porous media are fundamentally stable when the initial solution is diluted and the pH drops down below 8.

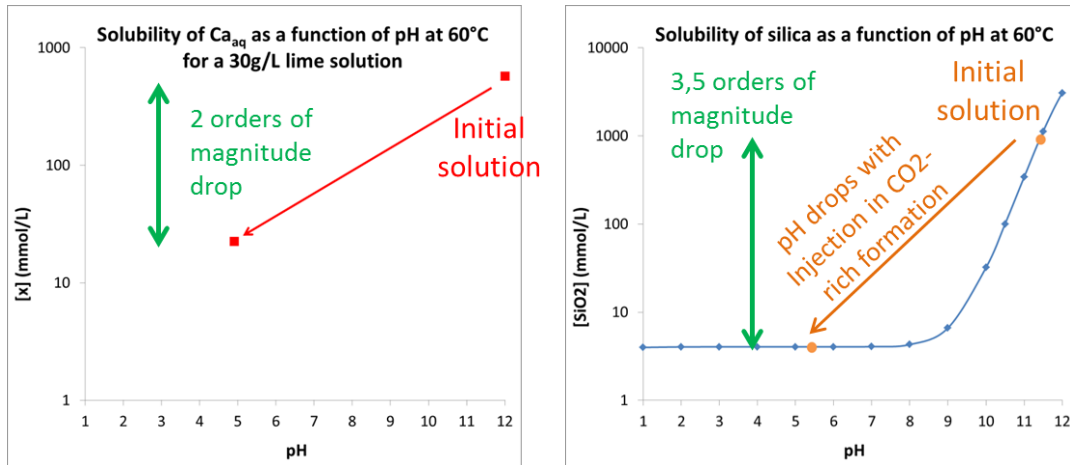


Figure 1: Solubility of Ca and SiO₂ as a function of pH.

The efficiency of carbonate vs. silicate solutions has been investigated recently (Ito *et al.*, 2014) by performing experiments in a bead pack (Figure 2). The reduction of the apparent permeability to CO₂ after precipitation of the injected solution is one order of magnitude larger for silicate solution compared to a lime solution. These observations confirm our reasoning.

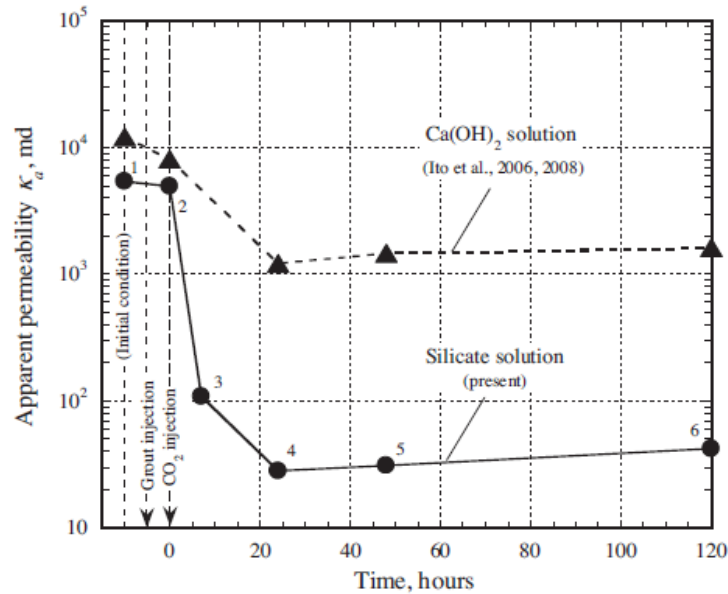


Figure 2: Reduction of the apparent permeability appearing larger when using silicate solution (Ito *et al.*, 2014). From experiments performed in a bead-pack.

In a very general way and in view of field applications, we can list a series of a priori advantages and disadvantages between processes involving carbonates or silicates (Table 1). Mixing at the surface may be easier for silicates because they are less sensitive to atmospheric CO₂; for injection issues; avoiding reaction in the well is possible for both processes; the kinetics of precipitation may be faster for carbonates than for silicates, although this should be compared more carefully; CO₂ gas is needed to lower the pH for carbonates, not necessarily for silicates; the stability w.r.t. pH

variations around neutral is better for silicates; carbonates are less costly; the environmental impact is very limited for both processes; and no strong safety issues exist for both processes.

Table 1: Comparison of precipitation processes involving carbonates and silicates.

	Carbonate	Silicate
Mixing at the surface	-	+
Reaction in the well	+	+
Kinetics	-	-/+
Need for CO ₂	yes	Not necessarily
Stability	-	+
Cost	+	-
Environmental impact	+	+
Safety	+	+

The theoretical general approach is to perform 2D reactive transport simulations at the well scale. These simulations should be validated first by 1D reactive transport simulations reproducing laboratory experiments, or some key aspects of laboratory experiments.

2 LITERATURE REVIEW

A literature review shows that silicates in porous media are used in the petroleum industry but also for other applications related to soil consolidation and civil engineering (e.g. Azeiteiro *et al.*, 2014). Besides these two domains, systems made of silica and an alkali metal (e.g. NaOH, KOH) are heavily used in chemical engineering to produce silica particles by precipitation, and nanoporous solids as catalysis support. For this domain, the related knowledge can be found (at least) in two reference books on the subject (Iler, 1979; Bergna and Roberts, 2006). An overview of the general mechanisms involved in the precipitation processes to form particles is given in Figure 3. Starting from a liquid state containing various complexes (described later), the decrease of pH induces the formation of oligomer, followed by the growth of primary particles. If the concentration of these particles is high enough (as the pH is further decreased), the growing aggregates percolate and forms a gel. The gel may precipitate to form solid silica-based porous nano-particles. The sodium silicate chemistry is rather complex and still not fully understood. Quite surprisingly, new precipitation processes to produce silica particles can still be found nowadays (Jung *et al.*, 2010). Unfortunately, as will be seen, some important aspects of interest for our application cannot be found as well.

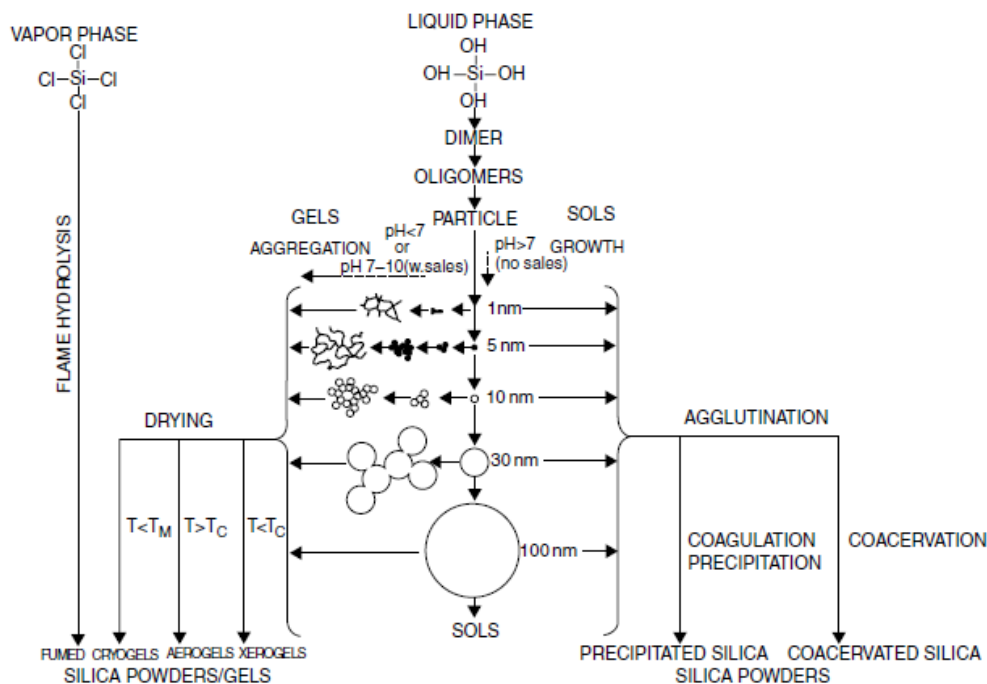


Figure 3: General overview of polymerization and precipitation of alkaline silica solution (Bergna and Roberts, 2006).

2.1 Sodium silicate solution as a flow diversion control in the oil industry

Sodium silicate is used for water control in oil reservoirs (Stavland *et al.*, 2011 and references therein). Combined with polymers, it has been used for well treatments or conformance control in order to reduce water production (Lakatos *et al.*, 1999, 2012) and more recently CO₂ gas losses (Lakatos *et al.*, 2014). In the latter, the treatment was applied in one well of the Becej field and effectively reduced considerably the gas losses. The addition of silicates in polymers (called silica-based gels) improves the gel strength and stability.

For in-depth placement and control, one tries to form a gel after the injection of a silicate solution. The main issues are the following:

- control the gelation time in order to reach a given (or the largest) distance around the well,
- choose an appropriate viscosity in order to generate reasonable pressure increase in the formation, below the fracking limit,
- because the initial solution is often a colloidal suspension containing already particles, an additional issue is to avoid plugging by collective aggregations in the restrictions of the pore network (pore throats) if these particles are large.

The success of the process is quantified by a water mobility reduction factor, comparing the initial permeability of the porous media to that after gelation. But for placement in the formation at a given distance, one should avoid early gelation or precipitation during the injection, and different authors have investigated recently in detail the gelation kinetics as a function of different parameters: pH, dilution in water, dilution in HCl, NaCl salinity and presence of divalent ions. We report below many results that are of high interest for our process.

Dilution and pH

Since the pH is the main parameter triggering the gelation time, the pH was determined for different dilution with distilled water and/or HCl (Hamouda and Amiri, 2014). From the initial solution at pH=11.4 (note that its density is very large), the pH decreases only when a very large amount of water is added. We used this property to adjust the viscosity of the solution. Another useful curve is the pH when using an acid (HCl, Figure 5). As expected, stronger decreases are observed; with a larger Na-Si concentration, more acid is needed to lower the pH and the different curves appear to be coherent (e.g. the curve for a concentration of 6 can be deduced from the curve at a concentration of 3 by multiplying abscissa values by 2).

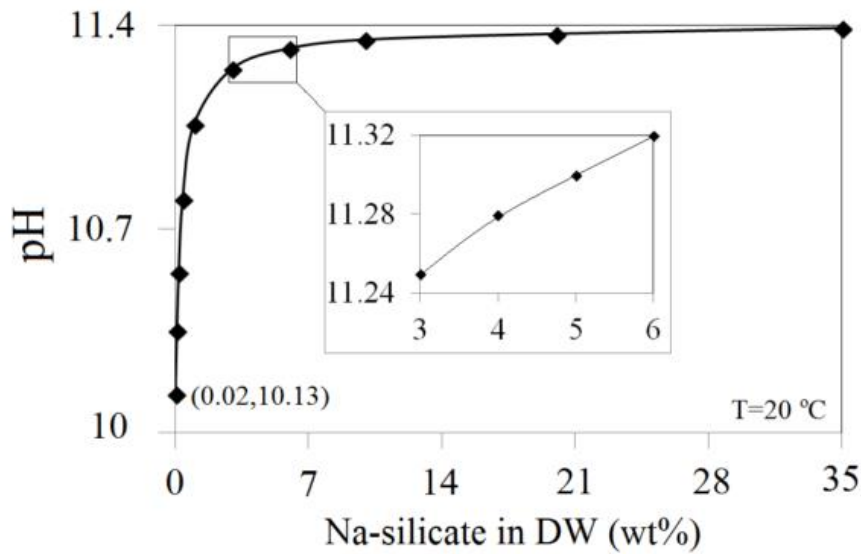


Figure 4: pH of different solution diluted in distilled water. The highest concentration corresponds to the initial solution provided by the manufacturer: Na-Silicate (Na_2OSiO_2) content of 35.7 wt%, molar ratio of 3.35, silicate (SiO_2) content 27.4 wt%, Sodium oxide (Na_2O) of 8.4 wt%, density of 1.368 g/cm³ at 20°C (Hamouda and Amiri, 2014).

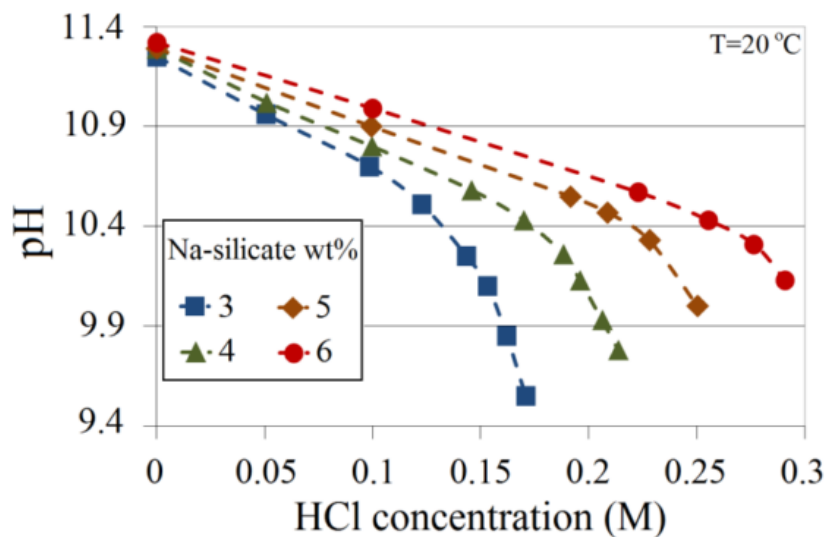


Figure 5: pH of different solutions diluted with hydrochloric acid (Hamouda and Amiri, 2014). The initial solution (HCl conc. of 0) at different Na-silicate concentration (from 3 up to 6) were obtained by diluting the solution provided by the manufacturer with distilled water (see Figure 4).

Gelation time

The gelation time is typically measured using a rheometer and is defined as the time at which rheological properties are stable. It was studied for the above mentioned solution (Figure 6). As the Na-Si concentration increases, the gelation time becomes very short below pH=10 (a few minutes). These graphs suggest that the gelation may be quasi-instantaneous when using concentrated solution. A more comprehensive explanation of gelation is given by Tognonvi et al. (2011b). The gelation time of an alkaline silica solution ([Si]=3.7 mol/l) diluted in HCl has been studied and the results reported either at a constant Si concentration or at a constant pH to observe the effect of these two parameters independently (Figure 7). The increase of gelation times for increasing pH is interpreted as a competition between poly-condensation reactions and the formation of silicate species due to the dissolution of particles. The decrease of gelation times for increasing concentration is due to a dilution effect, poly-condensation effects becoming more difficult when particles are more dispersed.

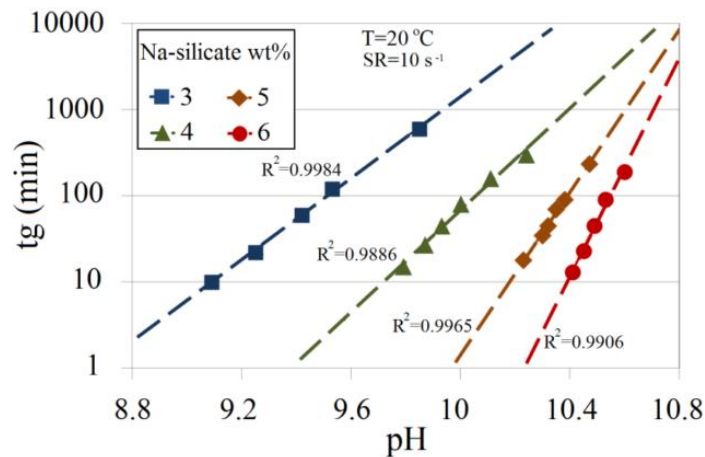


Figure 6: Gelation time t_g for the solution described in Figure 5 (Hamouda and Amiri, 2014).

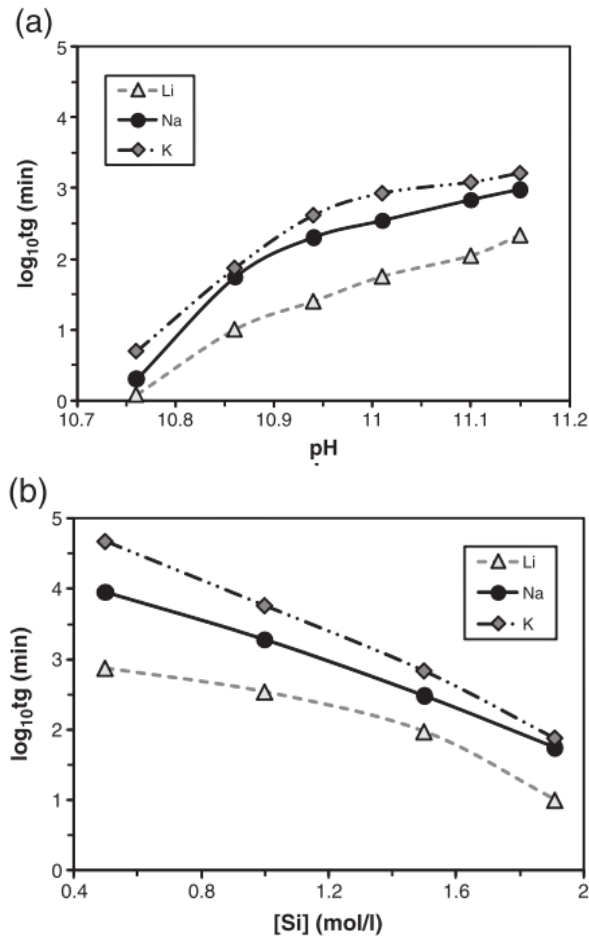


Figure 7: Effect of pH at constant silicon concentration [Si]=1.91 mol/l (a) and concentration at constant pH=10.86 (b) (Tognonvi *et al.*, 2011b).

Effect of temperature

The temperature effect on gelation times can be described by a Arrhenius type relationship - $\exp(E_a/RT)$ - where E_a is an activation energy (J/mol), R is the gas constant (8.314 J/mol/K) and T is the temperature in Kelvin. Above 40°C, it was found (Hamouda and Amiri, 2014) that the gelation time decreases with $E_a=70$ kJ/mol (Figure 8), in agreement with other work (when gathering all works, the range is 60-80 kJ/mol). Similarly for the precipitation rate, an Arrhenius relationship was also chosen with an activation energy of -49.8 kJ/mol in the range of temperature relevant for geologic storage (Ito *et al.*, 2014). A representation of such exponential increase indicates that the gelation time may increase by a factor of 5 between 40 and 60°C, and the precipitation rate by a factor of 11 (Figure 9).

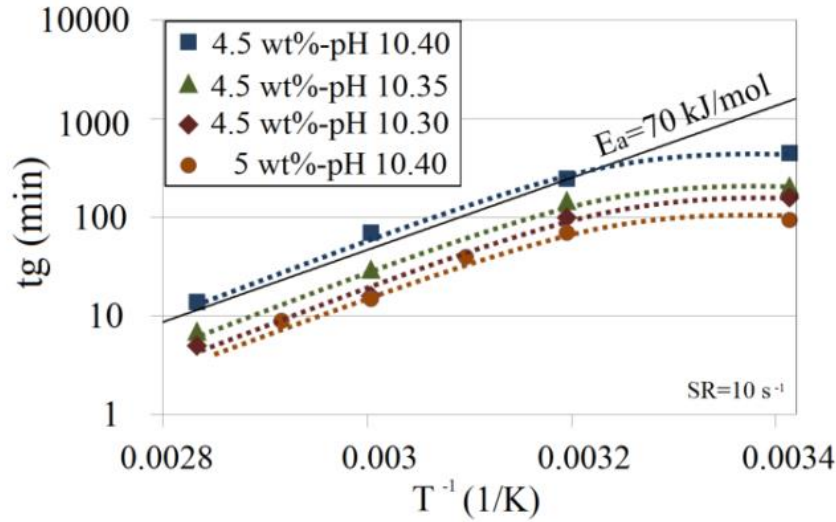


Figure 8: Range of investigated temperature in °C: from 21 up to 84°C. (Hamouda and Amiri, 2014)

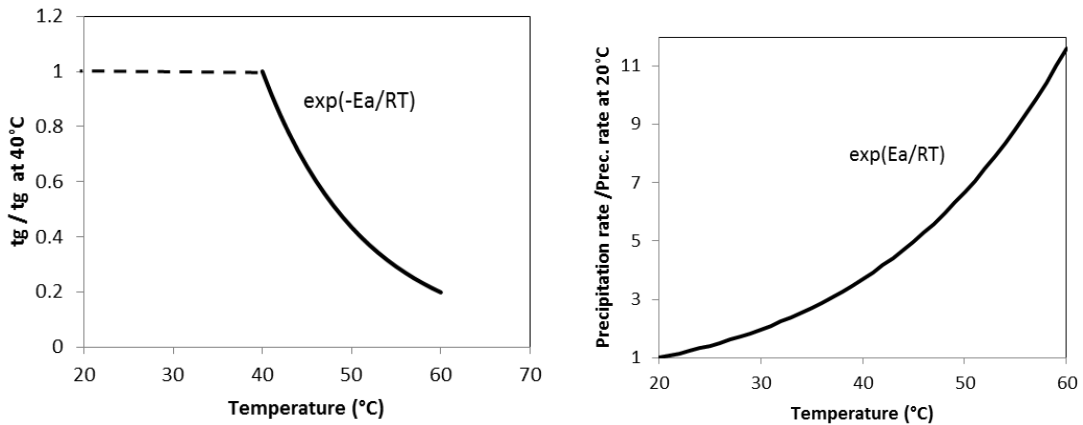


Figure 9: Graphical representation of the variation of gelation time t_g and precipitation rate in the range 20-60°C. For gelation $E_a=70\text{kJ/mol}$, for precipitation $E_a=49.8\text{kJ/mol}$.

Effect of salinity

Similarly to clay suspensions, the presence of salt affects the gelation time or may even generate a gel. In general, dissolved salts tend to reduce repulsive forces between particles, depending also on their surface charges. It was found (Metin *et al.*, 2014) that the gelation time may be severely affected by dissolved salts in the usual range of interest in geological formations (Figure 10). However, in this case, the studied system is different: it is a suspension of non-porous silicate particles of size around 10 nm, in brines with different salinities. The gelation time decreases by several orders of magnitude. It was also observed that divalent ions (Ca^{2+} or Mg^{2+}) also impact the gelation time compared with NaCl brines (Hamouda and Amiri, 2014).

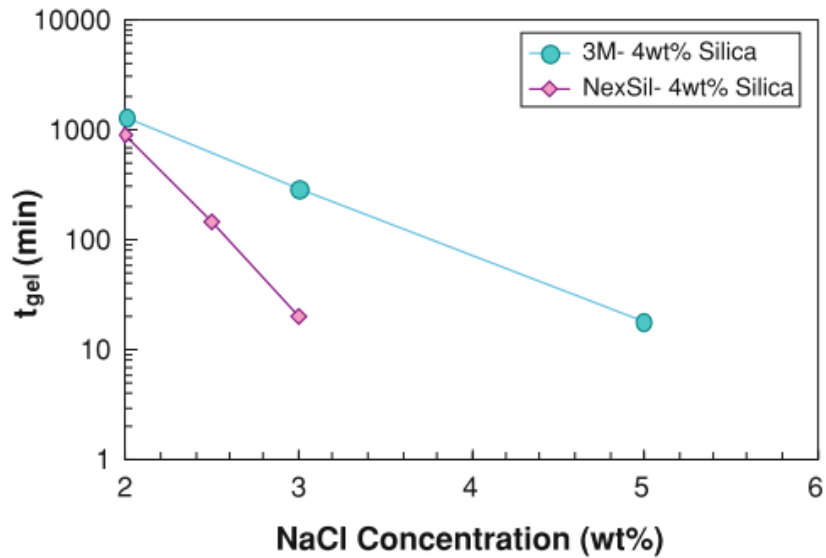


Figure 10: Gelation time for 2 suspensions of silicate nanoparticles in NaCl brine of different concentrations (Metin *et al.*, 2014).

2.2 Sodium silicate solution as a consolidation material

Precipitated silica could also be used as a consolidation material (Kouassi *et al.*, 2011). The study was conducted on sands following the experimental process depicted in Figure 11. A concentrated solution is diluted with acid, then with two types of silica sands, and finally dried. After acidification, the system forms a gel. After drying, a solid is formed binding the grains together, as shown by compressive strength tests. The generation of crystals is very slow (days up to 100 days). We understand this slow generation as due to atmospheric CO₂ inducing a reduction of pH and subsequent crystallization. These experiments show that the silica precipitates are linked to the solid surface presumably through Si-OH bonds. Images of dried precipitates in glass bead packs (Ito *et al.*, 2014) also suggest some interactions with the solid surface.

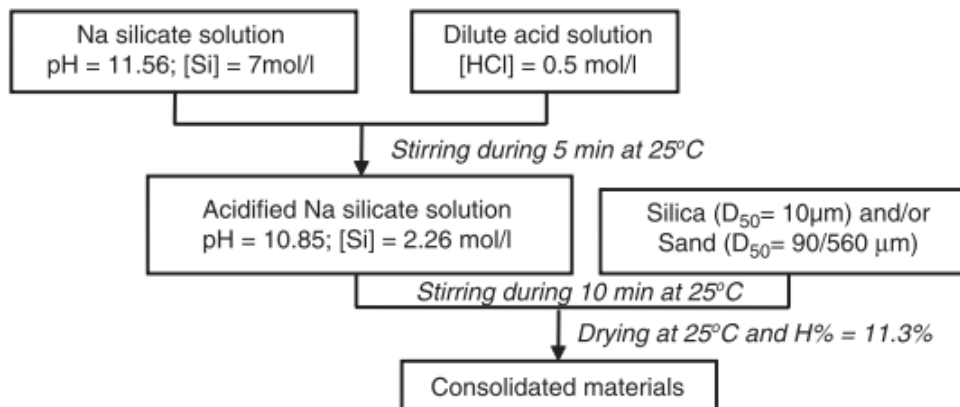


Figure 11: Experimental process to study consolidation of sands (Kouassi *et al.*, 2011).

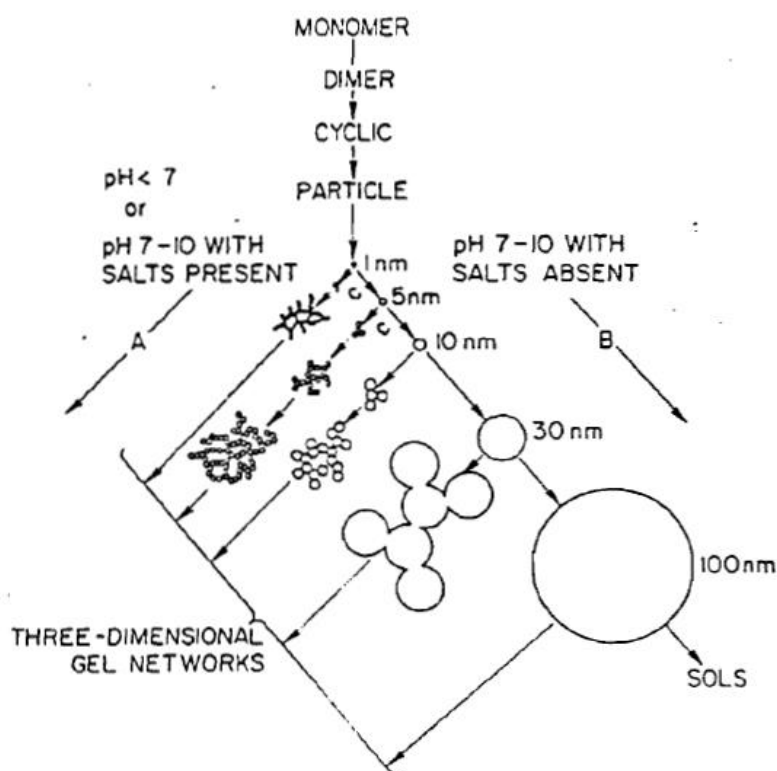
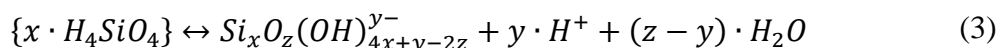


Figure 12: Polymerization and precipitation of alkaline metal silica solution (Iler, 1979).

2.3 Chemical characterization and speciation modelling of silico-alkaline solutions

Silico-alkaline solutions (SAS) are aqueous solutions containing high concentrations of SiO₂ and A₂O, where the alkaline element A is generally sodium (Na) or potassium (K). They are characterized by the molar ratio $\frac{SiO_2}{A_2O}$, denoted by R_m (commonly 1.6 to 3.9 in commercial solutions, see Iler, 1979). High silica solubility is only possible at high pH (see Fig.I-3 in Tognonvi, 2009), a striking feature of concentrated SAS.

Whereas diluted solutions (< 0,01 M Si) contain only the monosilicic acid H₄SiO₄(aq) and its associated anions H₃SiO₄⁻ and H₂SiO₄²⁻, SAS contain a variety of oligomers {x · H₄SiO₄}, with x up to 8, and their conjugated anions (Gaboriaud, 1999):



A general framework for the polymerization/precipitation process is depicted in Figure 12 (Iler, 1979) but more detailed descriptions have only been available recently. The structure of oligomers can be described from ²⁹Si NMR spectroscopy (Figure 13).

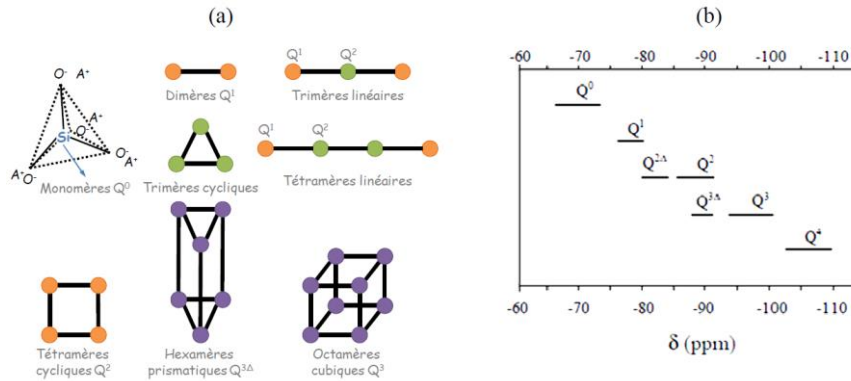


Figure 13: Silicic oligomer structures revealed by ²⁹Si NMR spectroscopy, where Q represents the SiO₄ tetrahedron (coloured points), Qⁿ denotes the structure type (n is the number of bonding O, n < 4), and δ is the observed « chemical shift » measured in ²⁹Si NMR spectroscopy (Prud'homme, 2011).

Solution speciation, i.e., the distribution at equilibrium of concentrations and activities of dissolved species, can be calculated at conditions (temperature T, pressure P, concentration) for which equilibrium constants are available. Provided that relevant data are known, it is the most straightforward and rigorous way to predict pH and composition evolution when mixing the SAS with other solution, and to calculate saturation with respect to solid phases, e.g., a silica phase likely to precipitate when the SAS is acidified, or a mineral phase with which the SAS is in contact in a reservoir. An example of common species distribution is represented in Figure 14. A relatively sophisticated model was given by Lagerström (1959) (see Table 5 in the paper). Much more recently, Felmy et al. (2001) elaborated a thermodynamic model, based on Pitzer's formalism for activity correction in solutions of high ionic strength (see their Table II for K_{eq} and Table III for Pitzer parameters). The same kind of approach was followed by Provis et al. (2005) (resp. their Tab.1 and Tab.2).

Gaboriaud (1999) called K_{x,y} the constant associated to equilibrium (3), that means:

$$K_{x,y} = \frac{(Si_xO_z(OH)_{4x+y-2z})^{y-} \cdot (H^+)^y}{(H_4SiO_4)^x} \quad (4)$$

where (E) denotes the activity of a species E, and if water activity (H₂O) is assumed to be 1. He showed that :

$$\log K_{x,y} = y \cdot \log K_{1,1} + (1 - x) \cdot \log K_s \quad (5)$$

where K_s = (H₄SiO₄) is the solubility of silica :



Appropriate values for K_{x,y} must be adjusted to take into account the high concentration character (high ionic strength), and a convenient activity model (Pitzer). Therefore Gaboriaud (1999) proposes the values tabulated in Table 2 for SAS at R_m = 2, and in Table 3 for SAS at R_m = 3. The use of these K_{x,y} values is subordinated to the use of the Pitzer's activity model with parameters given in the same document.

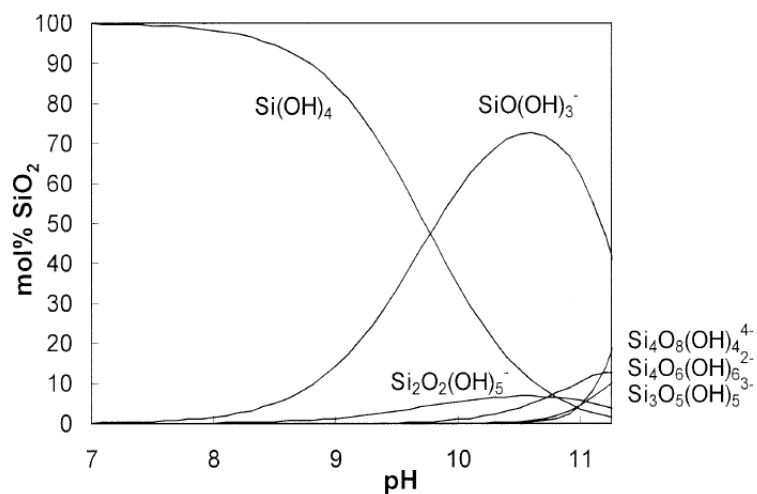


Figure 14: Distribution of the most abundant silicic species, at 25°C and at equilibrium with amorphous silica (Dietzel, 2000).

Table 2: Value of $\log K_{x,y}$ for $R_m = 2$ (Gaboriaud, 1999). Values indicated in bold character were modified with respect to eqn (5).

Charge Espèce y	Log ($K_{x,y}$)					
	monomère x=1	dimère x=2	trimère x=3	tétramère x=4	hexamère x=6	octamère x=8
0	0	2,7	5.4	8,1	13.5	18.9
1	-9,8	-7,1	-4,4	-1.7	3.7	9.1
2	-24,0	-19,8	-15,3	-11.5	-6.1	-0.7
3		-33,7	-28,6	-24,0	-15.9	-10.5
4			-44,6	-37,7	-30,3	-20.3
5					-44,3	-35,7

Table 3: Value of $\log K_{x,y}$ for $R_m = 3$ (Gaboriaud, 1999). Underlined values were modified, additionally to those already indicated in the previous table.

Charge Espèce y	Log ($K_{x,y}$)					
	monomère x=1	dimère x=2	trimère x=3	tétramère x=4	hexamère x=6	octamère x=8
0	0	2,7	5.4	8,1	13.5	18.9
1	-9,8	-7,1	-4,4	<u>0,6</u>	3.7	9.1
2	-24,0	-19,8	-15,3	<u>-12,0</u>	-6.1	-0.7
3		-33,7	-28,6	-24,0	<u>-16,5</u>	-10.5
4			-44,6	-37,7	-30,3	<u>-24,4</u>
5					-44,3	-35,7

Table 4: Silico-alkaline solutions for which Gaboriaud (1999) experimented acidification.

SiO ₂ mol	SiO ₂ /Na ₂ O mol ratio (R _m)	Na ₂ O (g) for 1 mol SiO ₂	dissolved mass g	SiO ₂ /Na ₂ O mass ratio
0,375	2,0	30,99	91,07	1,94
0,75	2,0	30,99	91,07	1,94
1,5	2,0	30,99	91,07	1,94
0,375	3,0	20,66	80,74	2,91
0,75	3,0	20,66	80,74	2,91
1,5	3,0	20,66	80,74	2,91

Gaboriaud (1999) used these values to simulate acidification of 6 distinct SAS (Table 4), which was also performed experimentally by incremental addition of 0,5 ml of 1 M HCl to 10 ml SAS (example Figure 15). Gelling (*gélification* in the figure) is a behavior observed at decreasing Si concentration (and pH) (Figure 16):

- **Domain A** : limpid, stable solution ;
- **Domain B** : gelling, transparent gel, stable except if T increase, or agitation, or water dilution ;
- **Domain C** : gelling, white gel, stable except if T increase or water dilution, ripening with time to form white grains that settle down ;
- **Domain D** : gelling, ripening irreversibly to solid.

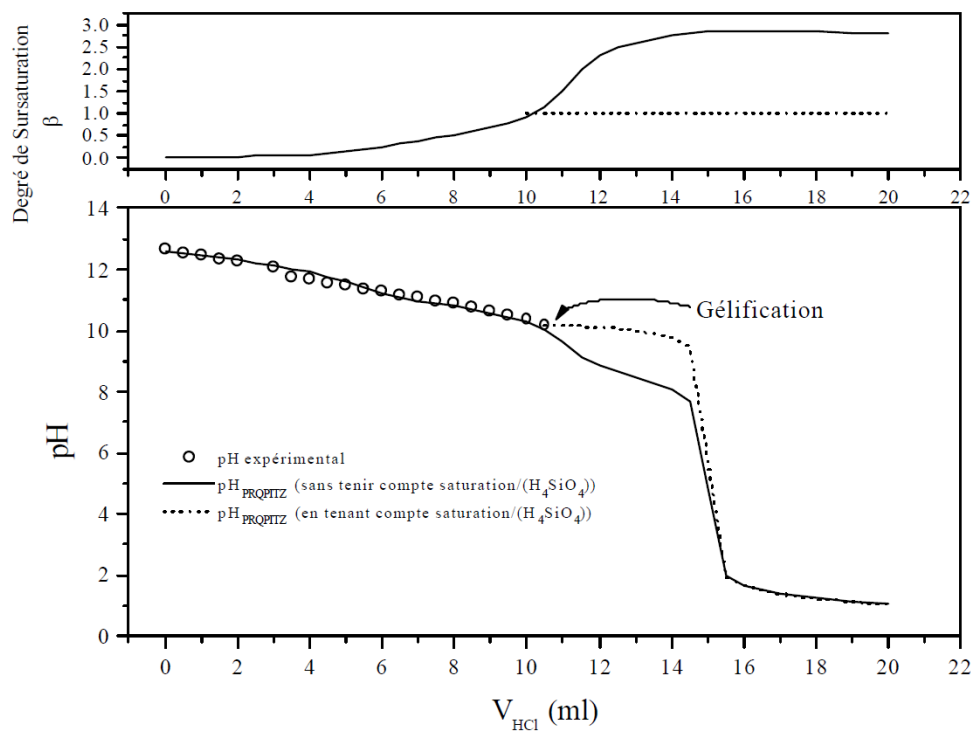


Figure 15: Acidification of a SAS containing 1,5 mol·l⁻¹ SiO₂ and 1 mol·l⁻¹ Na₂O (Gaboriaud, 1999). Two calculations were made, one preserves oversaturation with respect to silica (dotted line), the other respects equilibrium by silica precipitation (continuous line).

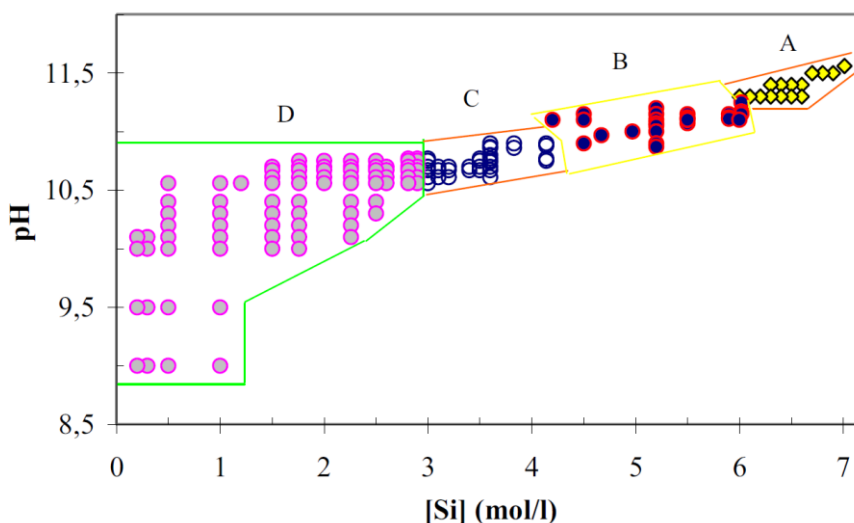


Figure 16: Various behavior of SAS observed at varying Si concentration and pH (Tognonvi, 2009). Domain A : limpid, stable solution ; Domain B : gelling, transparent gel, stable except if T increases, or agitation, or water dilution ; Domain C : gelling, white gel, stable except if T increases or water dilution, ripening with time to form white grains that settle down ; Domain D : gelling, ripening irreversibly to solid.

Oligomers are described as purely Si-O-H structures in all the publications we could refer to, except Tognonvi (2009) and (Tognonvi *et al.*, 2010) who introduced Na-Si-O-H structures to account for the observed gels that appear from Na-Si waterglass (Figure 17). Their approach combined small-angle X-ray scattering (SAXS) to ²⁹Si NMR spectroscopy. The concentrated sodium solution had the following characteristic: pH=11.56, [Si]=7mol/l, Si/Na atomic ratio=1.71. Initially at the highest pH (11.56), the identified species is a Si₇O₁₈H₄Na₄ neutral complex (Figure 17). As the pH decreases with water dilution, the above neutral complex is dissociated progressively into (Si₇O₁₈H₄Na_{4-n})ⁿ⁻ and Na⁺ ions. The same authors also studied the complexes formed during dilution with hydrochloric acid (Tognonvi *et al.*, 2011a). In particular, in the pH range 9-10.75 and Si concentration between 0.2-2.9 mol/l, irreversible gels are formed and solids are generated. According to this interpretation, the Si₇O₁₈H₄Na₄ complex and its associated anions (equilibria [5] to [8] in Tognonvi *et al.*, 2010) contain the major part of the dissolved silica in concentrated SAS at high pH. Unfortunately, they did not provide the K_{eq} constants attached to these equilibria.

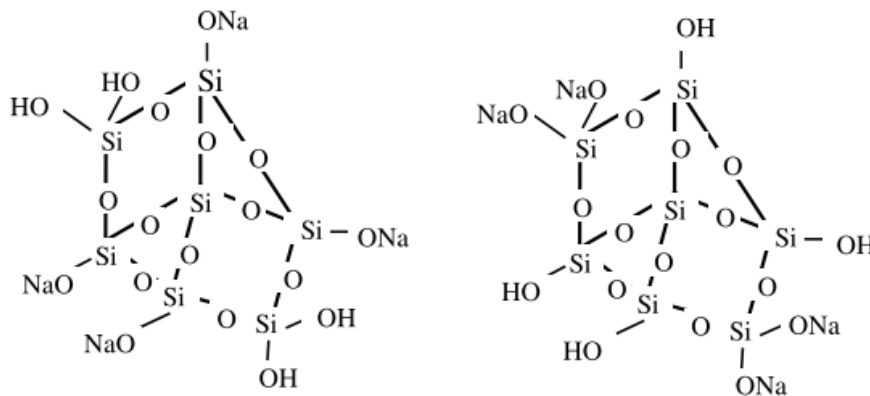


Figure 17: Structure of two possible $\text{Si}_7\text{O}_{18}\text{H}_4\text{Na}_4$ complexes compatible with the NMR and SAXS measurements (Tognonvi *et al.*, 2010).

2.4 Physical properties of sodium silicate alkaline solution

Viscosity and density can be found in individual studies. Charts showing general trends are available since 1952 (Vail, 1952). For viscosity (Figure 18), we observe a sharp decrease in a narrow range of Na_2O content for Na silicate alkaline solution diluted in water. Similarly, the pH is not sensitive to water dilution (Figure 19) unless one uses very large dilution ratios. Note however that the pH may reach a maximum for high $\text{SiO}_2/\text{Na}_2\text{O}$ ratio (e.g. 3 in Figure 19).

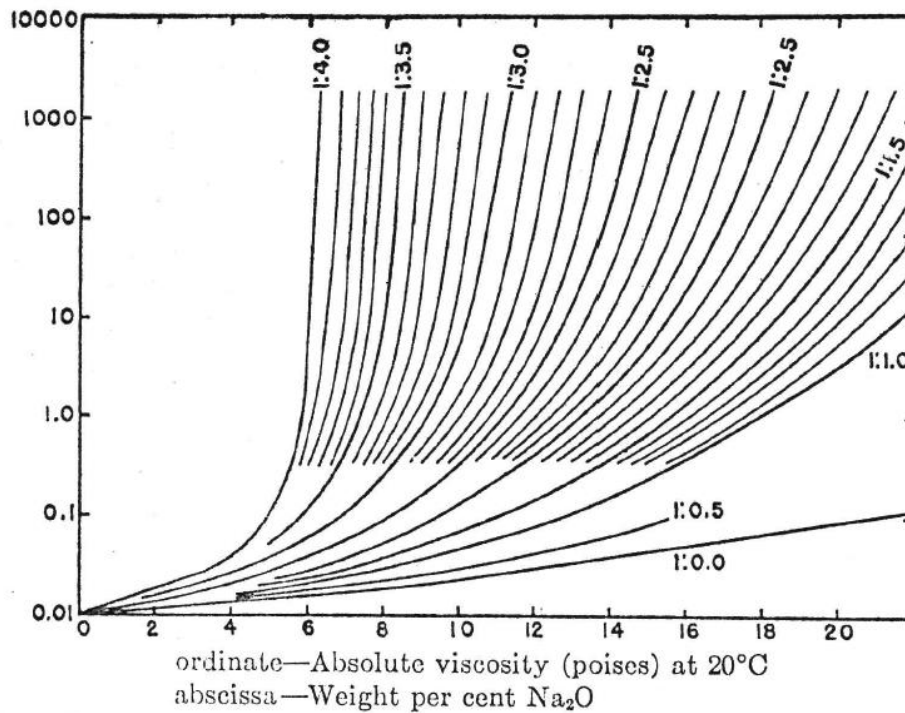


Figure 18: Viscosity chart (Vail, 1952) at 20°C for constant Na₂O /SiO₂ ratio (by weight) as a function of Na₂O content; the solution is diluted with water (Vail, 1952).

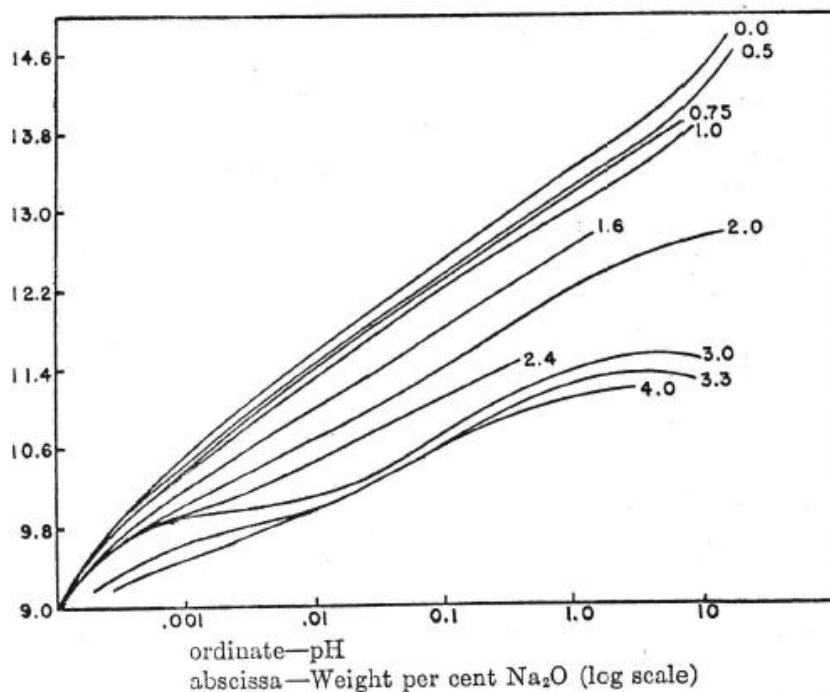


Figure 19: pH for constant SiO₂/Na₂O ratio (by weight) as a function of Na₂O content; the solution is diluted with water (Vail, 1952).

3 EXPERIMENTAL RESULTS

3.1 Solution characterization

Sigma-Aldrich solutions

The first tests were performed using a solution provided by Sigma-Aldrich (ref. 33844, main characteristics listed in Table 5). Although it is not planned to be used in field tests, CO₂ experiments have been performed with this solution. Viscosity and specific gravity for different water dilutions are plotted in Figure 20 and Figure 21. Excluding the points for the pure solution (100%), the viscosity variations can be modeled using exponential functions for viscosity at each temperature (20 and 40°C). This is in agreement with the general trends discussed above (Vail, 1952): at large dilution, the viscosity is described by an exponential law up to a certain limit at which it increases sharply. For density, a linear relationship can be used for both temperature (20 and 40°C). We chose to work with a solution diluted at 50 wt% in order to have a reasonable viscosity. This dilution does not significantly decrease the pH, as expected.

Table 5: Characterization of the Sigma-Aldrich solution (SA solution).

Sigma-Aldrich solution		Source
SiO ₂ content	26.7 wt%	Manufacturer
SiO ₂ content	26.1 wt% 6.04 mol/l	Measured
SiO ₂ /Na ₂ O	2.2	Measured
Na ₂ O	11.8 wt% 2.645 mol/L	Measured
pH	11.9	Measured
Specific density	1.39 g/cm ³	Manufacturer
	1.47 g/cm ³ at 20°C	Measured
Viscosity	233.5 mPa.s at 20°C	Measured
	78.6 mPa.s at 40°C	Measured

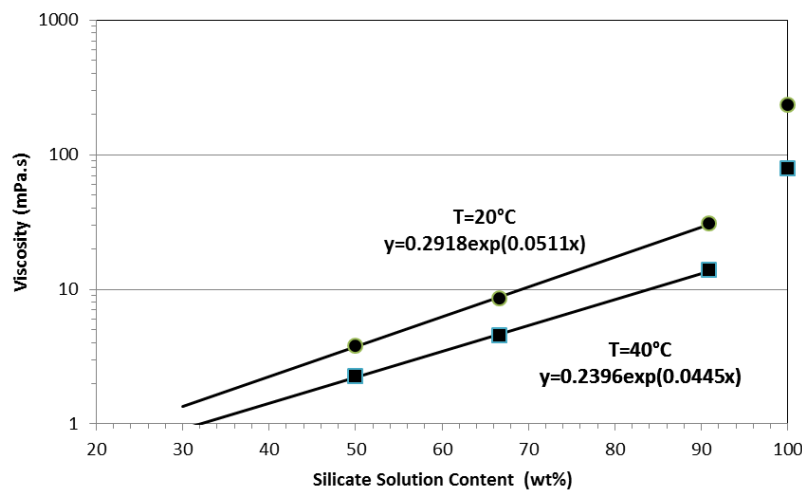


Figure 20: Viscosity of water diluted solution for two temperatures. The solution considered here is the SA solution.

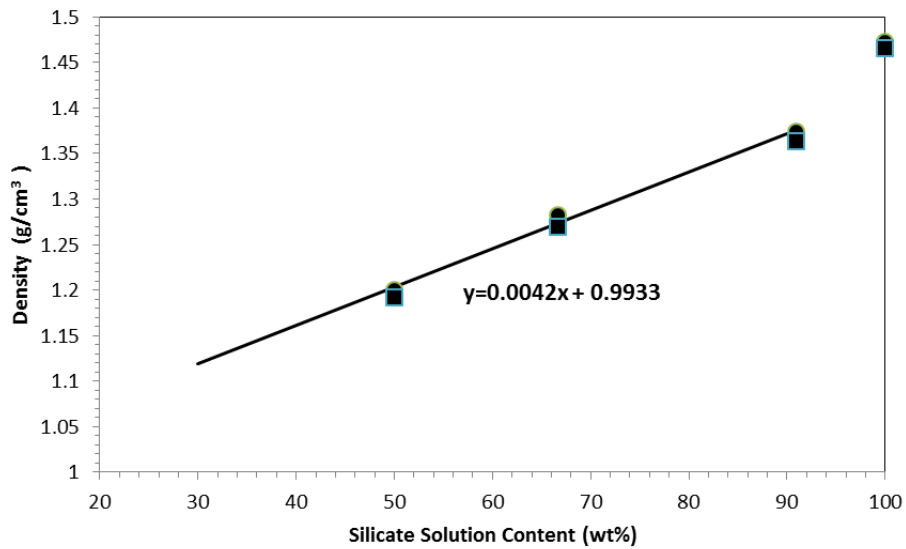


Figure 21: Density of water diluted silica solution at 20°C and 40°C. The solution considered here is the SA solution.

Woellner solutions

The solutions planned for field tests are provided by Woellner, a leading manufacturer of silicates (Table 6). Among the 4 products available, we chose a potassium silicate with the lowest viscosity, BetolK28T. Diluted at 50wt%, the viscosity is reduced to 1.1 cP at 40°C, with a density of 1.11 g/cm³.

Table 6: Characterization of Woellner solutions (SA solution).

Product Name	SiO ₂ %	Na ₂ O %	K ₂ O	Molar ratio	Viscosity (cP)	Density	pH
Ligasil 39	27.5	8.3	0	3.47	100	1.37	11.3
NaSil HK35	26.1	7	0	3.85	150	1.32	11.3
Betol K35T	23.9	0	10.9	3.43	55	1.32	11.0
Betol K28T	20.5	0	8.2	3.92	28	1.25	10.8

3.2 Batch experiments: precipitation using CO₂

Several batch experiments were performed with the SA solution to see if precipitates are generated. In a reactor maintained at 40°C, different diluted solutions were placed in contact with CO₂; the reactor is then closed and the pressure recorded (Figure 22).

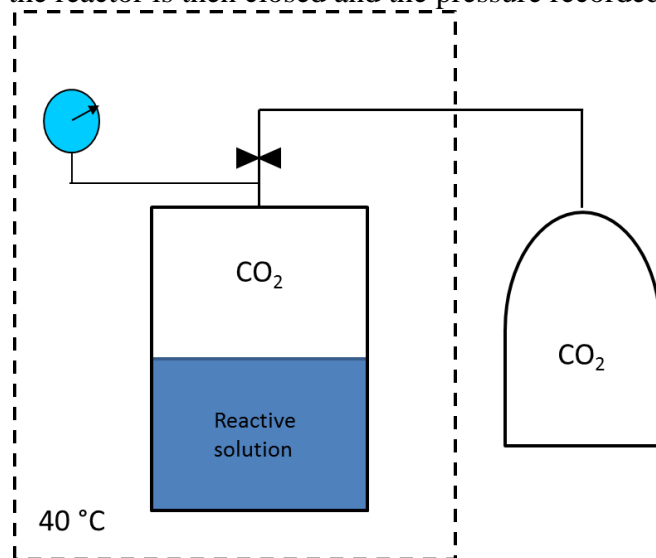


Figure 22: Schematic of batch experiments with CO₂. The reactor is maintained at a constant temperature and the gas pressure recorded.

Table 7: Parameters of batch experiments. The solution is the SA solution described in Table 5.

Batch exp. #	Dilution	Volume ratio, gas to total liquid (%)	Pressure (bar)	Final pH	Observation
1	Sol 100 g Water 10g	40	50	Not measurable	Reactor totally filled with solids
2	Sol 100g Water 10g	40	10	11.9	Thick solid film at the surface 3.82% heavier
3	Sol 100g Water 10g	40	10 bar CO ₂ 40 bar Argon	11.8	Thick solid film at the surface 3.82% heavier
4	Sol 50g Water 50g		50 bar CO ₂	Not measurable	Reactor totally filled with solids

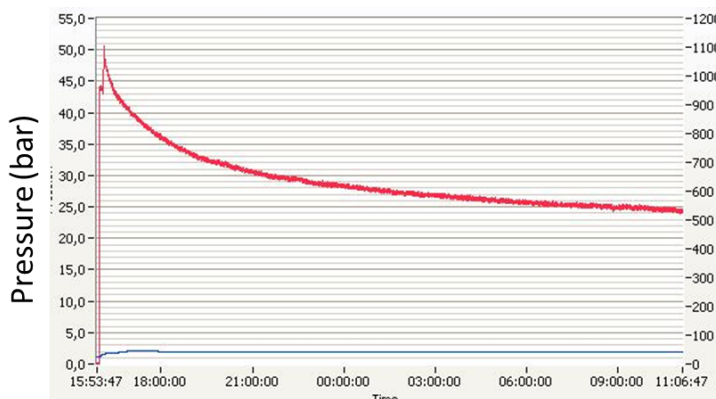


Figure 23: Batch experiment 1; after 19 hours, the reactor was full of solids, and no water was left; the solid contains trapped water that was measured with NMR. 25 bar of CO₂ remains in excess.

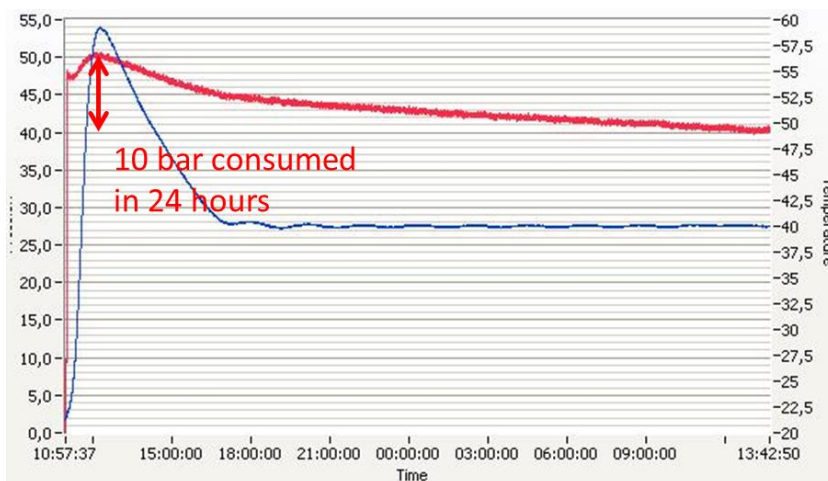


Figure 24: Batch experiment 3; after 24 hours, the 10 bar of CO₂ have been completely consumed, and a solid carbonate phase surrounded by silica gel has formed on top of the remaining water glass solution.

The run products for experiments 1-3 (10% water, 90% water glass solution) are about 4 wt% heavier than the initial solution introduced in the reactor, which indicates that CO₂ has been trapped in the solid run products. It indeed appears that solid carbonate phases are formed as well as amorphous silica gel, as it is indicated by the presence of a solid white precipitated product surrounded by the transparent silica gel. This observation is confirmed by XRD data (Figure 25), which indicates the presence of two different sodium carbonates, one being hydrated and having thus a higher molar volume.

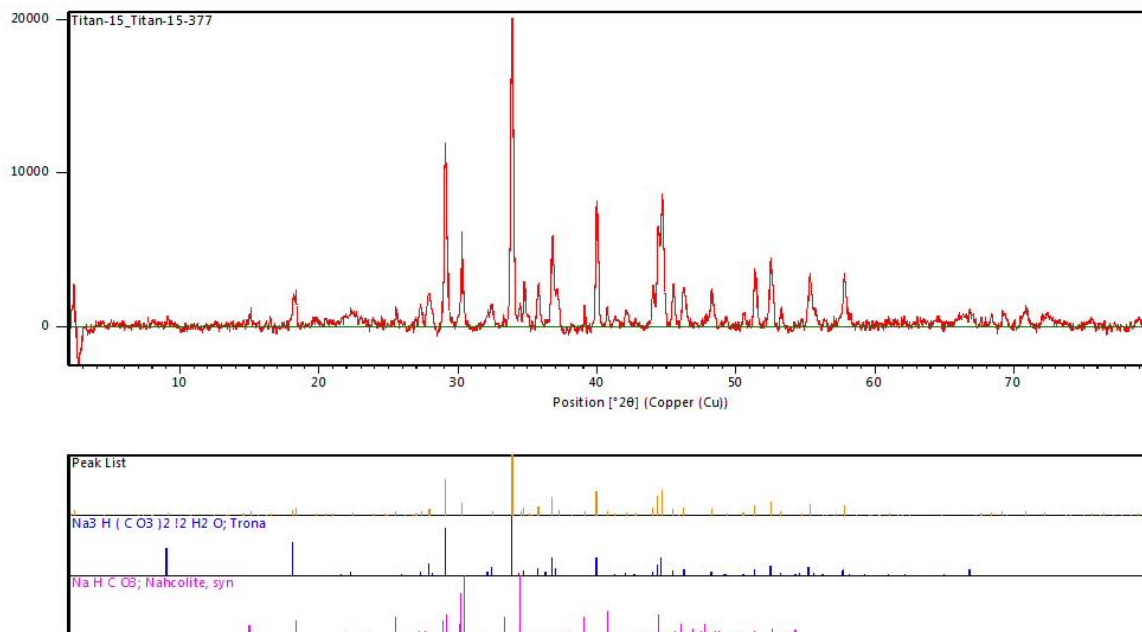


Figure 25: XRD spectrum of experiment 3 : anhydrous (nahcolite), but mostly hydrous sodium carbonates (trona) have formed within the run products, trapping the CO₂ and potentially increasing the molar volume of the amorphous silica gel.

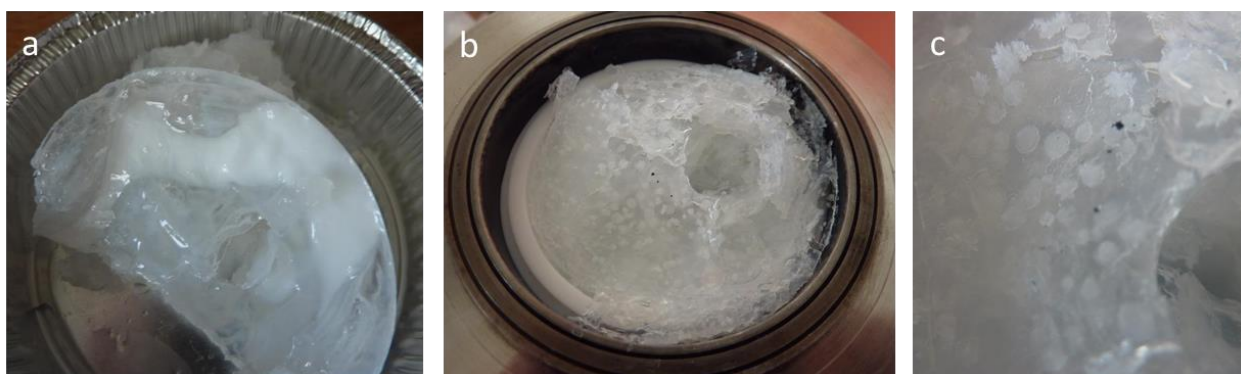


Figure 26: (a) Run products of experiment 2; silica gel is observed around a more solid white phase, formed of carbonates. (b)-(c) Run products of experiment 4. White centimeter-sized phases, which we identify as carbonates, can be observed in the silica gel.

It should be noted that the silica gel is extremely hydrated, and the water linked to the silica can apparently trap dissolved CO₂ within its matrix. Indeed, under 50 bar of CO₂, experiment 1 (90% water glass solution, 10% water) showed an increase of mass of 4 wt% in the run products. Under the same pressure of CO₂, experiment 4, which had more water in the reactive solution (50%/50%) showed an increase of mass of 10%. Since experiment 4 had less Na available to form Na-carbonates than experiment 1-3,

the excess amount of trapped CO₂ must have been dissolved in the gelified water of the solid silica phase.

To quantify the degree of hydration of the solid phase with a rudimentary method, 26.4 g of solid was placed over 24h at 60°C in an anhydrous environment. Only 6.75g remained after 24h. After 48h, 6.67 g. After a week, 6.52 g. In other words, it appears that around 75 wt% of the formed phase was composed of water. Since water actually represented around 83.5 wt% of the initial mixture (50% water glass solution, 50% pure water), it represents around 75.9 wt% of the run product incorporating trapped CO₂. This suggests that the residue remained feebly hydrated (0.9 wt%) and that the carbonates formed remain stable.

Hydration can also be quantified using low field NMR techniques. This was performed for the solids of experiment 1, using a solution containing less water. From the T₁-T₂ maps, we see that the T₂ relaxation times of the water is small (about 20 ms, main peak), indicating a high degree of confinement. This is also confirmed by a T₁/T₂ ratio of 2, a clear signature of water confined in a porous media and in interaction with a solid. The secondary tail at larger relaxation values (T₂ ~ 300 ms) may be due to water at the external surface of the solids. Quantitatively, the total mass of the sample was 3141.2 mg, and the measured mass of water by NMR was 192.8 mg, thus representing only 6% of the total mass. However, uncontrolled drying occurred for this sample.

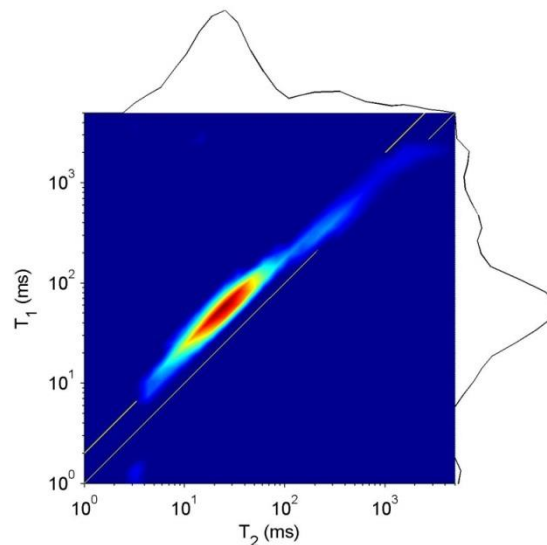


Figure 27: Low field NMR relaxation time T₁-T₂ maps for the water present in the precipitated “solids”. Lines indicate a T₁/T₂ ratio of 1 and 2.

3.3 Experiments in porous media with CO₂

An experiment was performed on a sand pack made of natural quartz grains (100-160 μm size). The protocol was the following:

- After saturation with 20 gr/l NaCl brine, measure permeability
- Inject the reactive solution in the column and monitor the pH at the outlet; stop when the pH has reached the value of the solution,
- Flush all tubing and end-pieces with brine,
- Flush all tubing and end-pieces with CO₂,
- Inject CO₂ through the column (24 hours) and measure the amount of solution left in the column,
- Inject brine to remove the reactive solution and CO₂ left,
- Measure the brine permeability.

It is designed to observe the change of permeability to water due the precipitation/adsorption of the reactive solution in the column. Potential artifacts due to plugging the inlet/outlet tubing are avoided when following the above protocol, and the design of the end-pieces of the cell has two entries available to allow flushing of the inlet/outlet faces of the sample (Figure 28). The pore pressure can be set by a back-pressure regulator. X-ray CT scanning has also been performed to observe the change of porosity along the column.

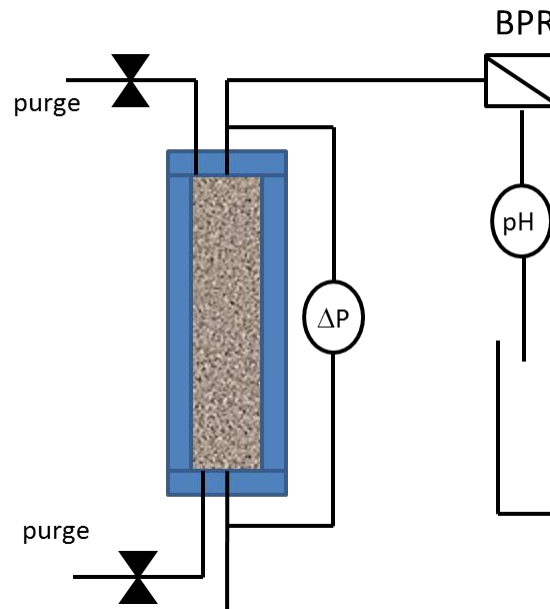


Figure 28: Schematic of the experimental set-up for testing reactive solutions in porous media. The column has an inner diameter of 28.4 mm and the sand-pack has a length of 140 mm (maximum).

Using the SA solution diluted with water (50wt%), the permeability decreased from 3220 mD down to 565 mD with little change of porosity (47%).

Using the SA solution diluted with water (50wt%), the CO₂ was continuously injected at a flow rate of 100ml/hr (at 10 bar). After CO₂ breakthrough, the liquid saturation was 67% and no further liquid production was observed. After flushing with brine and returning to 100% brine saturation, the permeability decreased from 3220 mD down to 565 mD with little change of porosity (47%), not detectable by CT scan (not shown). The continuous flow of CO₂ along the sand-pack corresponds to a situation in which the gas is in excess. For this solution, CO₂ at 10 bar does not allow strong precipitation (presumably), as observed in batch experiments.

A similar experiment was performed again using BetolHK35 solution diluted at 50wt% (same sandpack). However, the pore pressure was set at 50 bar (40°C). In this case, the CO₂ injection was impossible after 10 min of flushing (and after breakthrough). The sand-pack was totally plugged and no water permeability could be measured.

3.4 Precipitation using CO₂: conclusions

Using CO₂ to precipitate silica is an efficient means to form various solids at high CO₂ pressure. However, the reaction kinetics are fast and difficult to control. In addition, there is no theoretical basis to predict the run products. In a porous media (sand-pack), the decrease of permeability is moderate (a factor of 6) at low pressure (10 bar). At higher pressure (50 bar), the porous media is plugged and the permeability is not measurable (with a standard device; the permeability could be reduced to extremely low values smaller than 1 μD, but this not known).

Based on these observations and especially in view of the lack of possible control of the kinetics of precipitation, it was decided to explore a different option: use of a weak acid to initiate a precipitation the kinetics of which are compatible with field operations.

3.5 Batch experiments: precipitation using acetic acid

The solution used in these experiments is Betol K28T diluted with water (50wt%). Following the methodology of Tognonvi (2009), we tested several mixtures of diluted Betol and acetic acid (1M), similar to vinegar. Precipitation was qualitatively observed for various fractions of diluted solution and acid at 40°C (Figure 29). When enough acid is present, solid precipitates are observed after a variable time and these solids cannot be dissolved again back into water. If the acid content is too low (not shown), the gel is weaker and reversible. These tests allowed 3 acid concentrations to be tested in more detail using rheological and NMR measurements, as described in the next section.

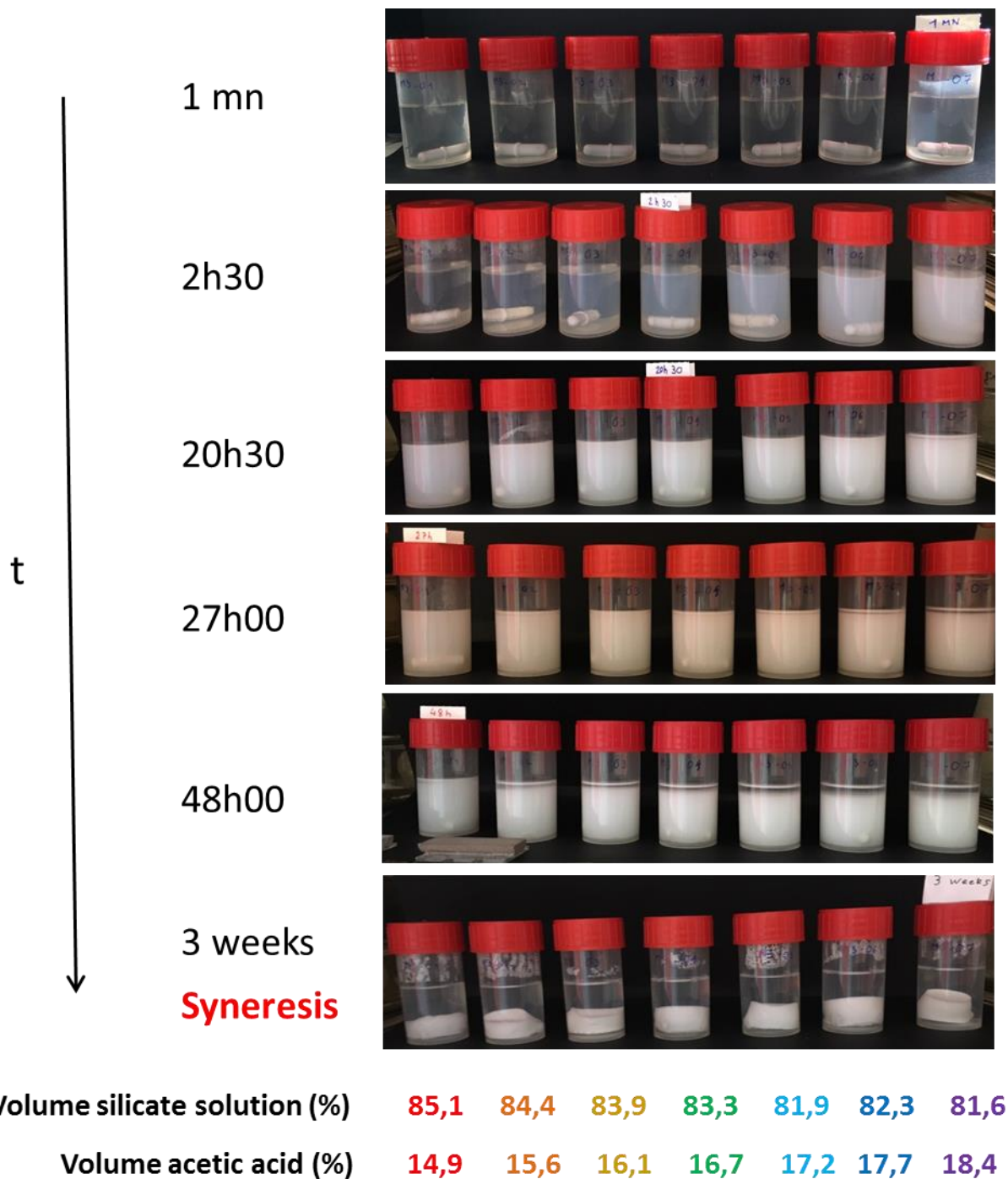


Figure 29: Precipitation experiments with acetic acid (1M) at different times. Solution: Betok28T diluted with water (50wt%).

3.6 Measurements of gelling times

The gelling times can be obtained very precisely from rheological measurements. The instrument used is a MCR300 from Physica. The geometry is a cone-plate maintained at 40°C using a Peltier set-up, together with a system minimizing evaporation and contact with air. The rheometer was operated in an oscillating mode at low frequency (1Hz) and small oscillating angle (<10°), yielding a shear rate as small as possible. Such protocols are common when studying polymers.

A typical result is shown in Figure 30. The purpose of the graph is to show the sudden increase in viscosity after 500 minutes, defining precisely the gelling time t_g (in this case 510 min); note that the viscosity value before gelling may not be accurate and it has been measured using another geometry.

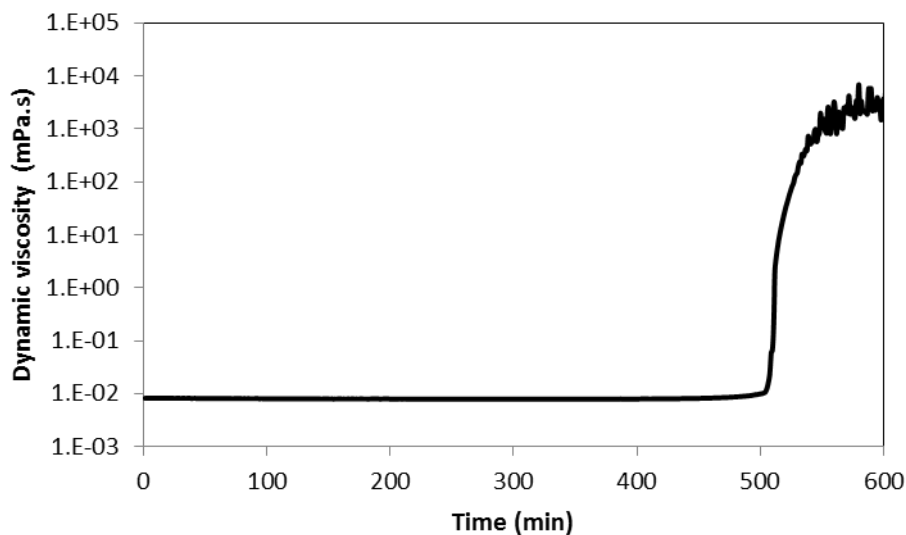


Figure 30: Evolution of the viscosity of a mixture diluted Betol K28T with 15.7wt% of acetic acid 1M. Temperature: 40 °C.

The viscosity measurements tend to indicate that no change in the mixture occurs before t_g but this is not true. Another useful method is to study the evolution of the water interactions within the mixture, and this is given by the NMR relaxation measurements as a function of time (Figure 31, performed with a 23 MHz apparatus from Oxford instrument); the T_2 relaxation time characterizing the mixture decreases progressively from the initial and maximum T_{2m} down to a plateau value T_{2p} . By comparing several viscosity and NMR measurements, we established that the abrupt change of viscosity corresponds to the time at which the relaxation time $T_2(t=t_g)$ is such that the relative variation of relaxation times is 0.235, i.e.,

$$\frac{T_2(t = t_g) - T_{2p}}{T_{2m} - T_{2p}} = 0.235$$

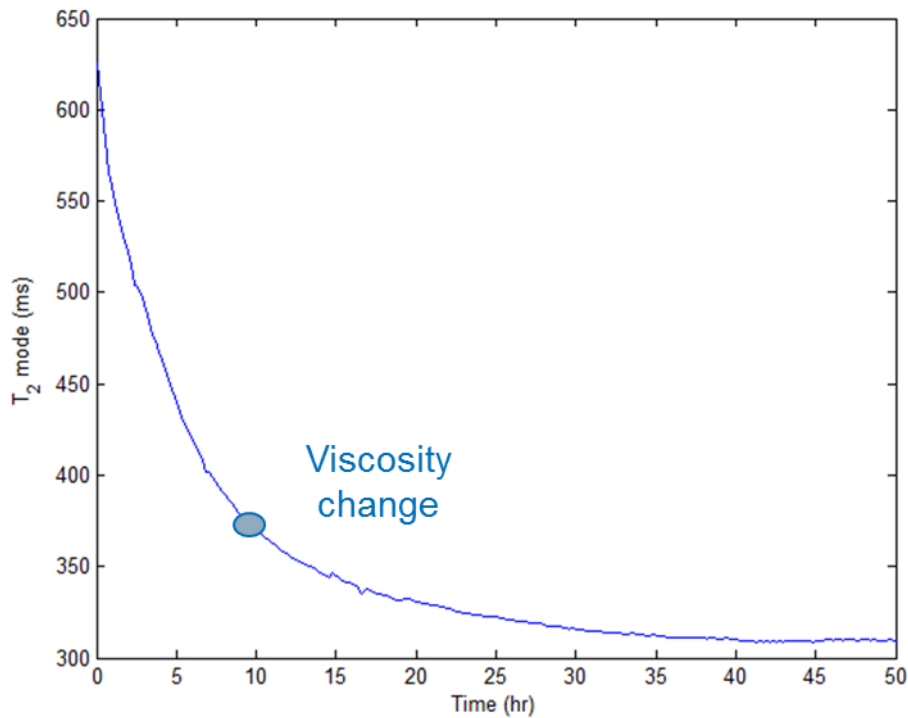


Figure 31: Evolution of the T₂ relaxation time for the same mixture as in Figure 30. The circle indicate the gelling time t_g (abrupt change of viscosity).

3.7 Effect of temperature and acid concentration

To study the effect of temperature on gelling times t_g, we use NMR measurements and the relationship between rheological and NMR relaxation measurements described above. NMR measurements are more convenient to use at high temperature and provide more information. The sensitivity can be described using an Arrhenius law (Figure 32):

$$t_g \propto \exp\left(-\frac{E_a}{RT}\right)$$

where E_a is an activation energy (J/mol), R is the gas constant (8.314 J/mol/K) and T is the temperature in Kelvin. From the data, we found E_a=80kJ/mol (Figure 32). Such a value is in agreement with literature as discussed earlier. Expressed in more practical units, such an activation energy means a strong dependence with temperature. For example, at 40 °C, we have a gelling time of 510 min (8.5 h), at 50°C, 193 min (3.2 h) and at 60°C , 77 min (1.3 h).

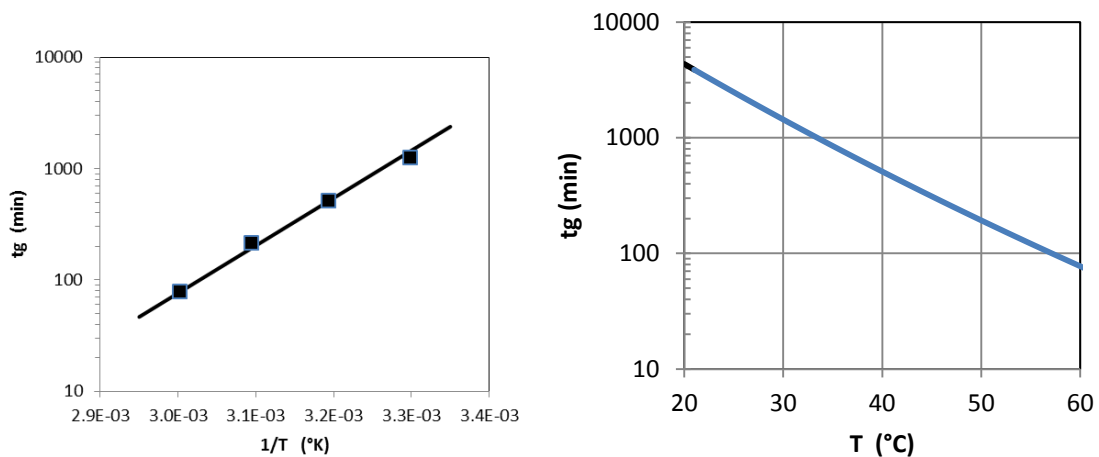


Figure 32: Gelling times determined by NMR as a function of temperature (data points at 30, 40, 50 and 60°C). BT28 solution diluted with 50wt% water. Acetic acid content: 15.7wt%.

Increasing the acid fraction above 15.7% decreases the gelling time by a factor of about 4.5 (Figure 33) but it is not possible to increase the gelling time by lowering further the acid fraction. Hence, it appears that, using acetic acid, a maximum and ideal value is reached (about 15.7%).

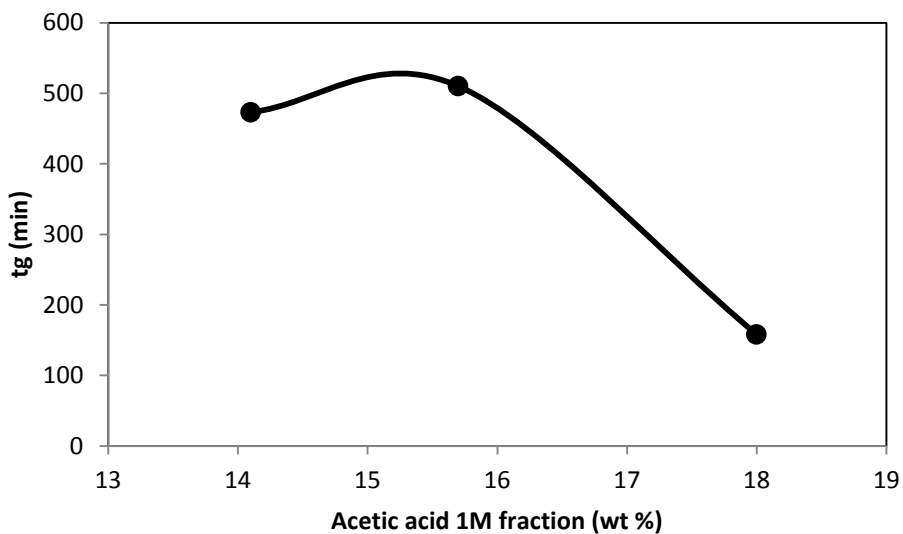


Figure 33: Gelling times as a function of acetic acid fraction at 40°C. Lowering the amount of acid in the solution does not increase the gelling times.

3.8 Experiments in porous media with acetic acid

The strength of the gel was tested in a porous media in a flooding cell (Figure 34). In a similar way to CO₂ injection experiments, we injected the mixture in different porous media. The samples are small plugs 2 cm in diameter and 3 cm long. The applied confining pressure was 80 bar, and the pore pressure was 20 bar. The protocol was the following:

- After saturation with 20 gr/l NaCl brine, measure the permeability to brine,
- Inject the reactive solution into the plug and monitor the pH at the outlet; stop when the pH has reached the value of the injected solution,
- Flush all tubing and end-pieces with brine,
- Wait for 24 hours or more,
- Inject brine through the tubing and end-pieces to verify that they are not plugged,
- Try to inject brine through the porous media.

This protocol was performed at 40°C. Several experiments of this type were performed and they all indicate that the porous media was severely plugged. For example, a pressure differential of about 20 bar could be applied to the plug before measuring a significant flow rate. Since the plug length was 3 cm, these tests give therefore a gel strength of the order 600 bar/m. This test was also performed with several differential pressure steps applied for longer period of times and it gave similar results. The tests were performed on a Vosges sandstone (50 mD) and a sample from the Becej field (5mD).

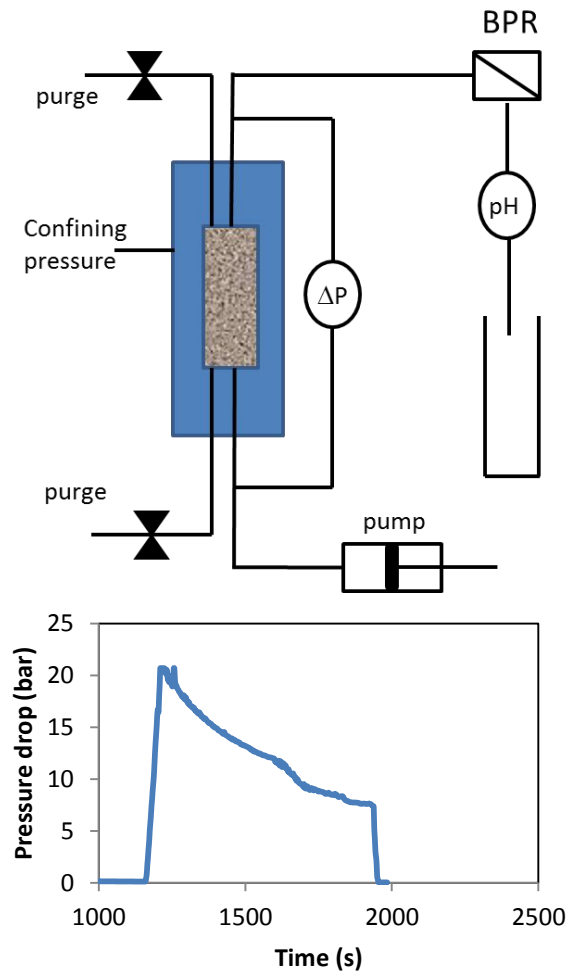


Figure 34: Simplified schematic of the experimental set-up for testing reactive solutions in porous media (left). The cell allows flushing all the tubing and end pieces to remove the reactive solution after flooding the porous media. The graph shows that a pressure differential of 20 bar could be applied before the gel breaks and allows brine to flow through the porous media.

4 SUMMARY AND CONCLUSION

In the framework of the MiReCOL three-year European project [1], a method for treating the surroundings of a well using a reactive suspension is studied. Among many possible choices, silicate based solutions were selected due to the following key qualities: high performance, long term chemical stability (w.r.t. acid), good injectivity (low viscosity and no particles) and no or little environmental impact.

Silica-alkaline solutions are aqueous solutions containing high concentrations of SiO₂ and A₂O, where the alkaline element A is generally sodium (Na) or potassium (K). Commercial stable solutions exist with a high molar ratio SiO₂/A₂O, spanning from 1.6 up to 3.9 with pH values above 11.5. When the pH is lowered either in contact with CO₂ or using an acid, silica precipitates to form particles. Below a pH of approximately 9 according to the solubility curve, the particles formed are stable and no back-dissolution is possible unless the pH is increased again. Hence, one expects a long-term stable chemical stability. Under certain circumstances, when induced in a porous media, this process has the potential to plug the formation around a well, to prevent gas or liquid flow through the treated formation.

An experimental investigation of the precipitation of commercial low cost sodium and potassium silicate solutions using a weak acid to lower the pH has been performed. Preliminary results using CO₂ indicate that the reaction kinetics are too fast and the plugging too strong to permit practical field implementation. Hence, laboratory experiments were performed testing various concentrations of acetic acid added to the commercial silica based solution, and estimating the bulk gelation times before the mixture became too viscous for injection. The impact of temperature was determined by performing experiments at 20, 40 and 60°C, with gelation times estimated between a few minutes up to 4 days. Multiple characterizations of the run products were performed using high resolution physico-chemical techniques. To follow the kinetics, several complementary techniques were used: rheological visco-elastic properties to observe the gel onset and NMR relaxation time measurements to follow the gradual increase of water interactions within the gel.

The ability of the precipitates to plug a porous media was tested on analog sandstone samples representative of CO₂ storage formations, as well as a sample from the Becej field (Serbia). With a viscosity close to water and no particles present in the liquid, injection of such products is possible in almost any permeable media. Using an optimum mixture tuned as described above, the solution is simply injected through the porous media and then left at constant temperature (e.g. 40 °C) for precipitation. After a few days, a breakthrough experiment is performed by increasing gradually the differential pressure across the sample. The results obtained so far indicate a very large strength of the order of 600 bar/m.

5 ACKNOWLEDGEMENTS

We thank Jorg Lind (Woellner company) for providing the various alkaline silicate solutions used during this project. Discussions with Sylvie Rossignol (University of Limoges) were also of great help for better understanding the chemical structure of the solutions.

6 REFERENCES

- Azeiteiro, L.C., Velosa, A., Paiva, H., Mantas, P.Q., Ferreira, V.M., and Veiga, R. (2014) Development of grouts for consolidation of old renders. *Construction and Building Materials*, 50, 352–360. Elsevier Ltd.
- Bergna, H.E. and Roberts, W.O. (2006) *Colloidal Silica: Fundamentals and Applications*. Taylor & Francis, 895 pp.
- Dietzel, M. (2000) Dissolution of silicates and the stability of polysilicic acid. *Geoch. Cosmoch. Acta* **64** (19), 3275-3281.
- Felmy, A.R., Cho, H., Rustad, J.R., Mason, M.J. (2001) An Aqueous Thermodynamic Model for Polymerized Silica Species to High Ionic Strength. *Journal of Solution Chemistry* **30** (6), 509-525.
- Gaboriaud, F. (1999) *Étude du rôle de l'ion alcalin au cours de la gélification des solutions silico-alcalines déstabilisées par addition d'ions calcium*. Ph.D Univ. de Bourgogne, 175 p.
- Hamouda, A.A. and Amiri, H.A.A. (2014) Factors Affecting Alkaline Sodium Silicate Gelation for In-Depth Reservoir Profile Modification. *Energies*, 7, 568–590.
- Iler, R.K. (1979) *The Chemistry of Silica. Solubility, Polymerization, Colloid and Surface Properties, and Biochemistry*. JOHN WILEY & SONS, 868 pp.
- Ito, T., Xu, T., Tanaka, H., Taniuchi, Y., and Okamoto, A. (2014) Possibility to remedy CO₂ leakage from geological reservoir using CO₂ reactive grout. *International Journal of Greenhouse Gas Control*, 20, 310–323. Elsevier Ltd.
- Jung, C.Y., Kim, J.S., Chang, T.S., Kim, S.T., Lim, H.J., and Koo, S.M. (2010) One-Step Synthesis of Structurally Controlled Silicate Particles from Sodium Silicates using a Simple Precipitation Process. *Langmuir*, 26, 5456–5461.
- Kouassi, S.S., Tognonvi, M.T., Soro, J., and Rossignol, S. (2011) Consolidation mechanism of materials obtained from sodium silicate solution and silica-based aggregates. *Journal of Non-Crystalline Solids*, 357, 3013–3021. Elsevier B.V.
- Lagerström, G. (1959) Equilibrium studies of polyanions. III. Silicate ions in NaClO₄ medium. *Acta Chimica Scandinavica* **13**, 722-736.
- Lakatos, I., Lakatos-Szabo, J., Tiszai, G., Palásthy, G., Kosztin, B., and Trömböczky, S. (1999) Application of Silicate-Based Well Treatment Techniques at the Hungarian Oil Fields. in: *Proceeding of the Society of Petroleum Engineers SPE 56739*.
- Lakatos, I., Lakatos-szabó, J., and Sciences, E. (2012) Reservoir Conformance Control in Oilfields Using Silicates : State-of-the-Arts and Perspectives. in: *Proceeding of the Society of Petroleum Engineers SPE 159640*.
- Lakatos, I., Medic, B., Jovicic, D., Basic, I., Lakatos-Szabo, J., and Tiszai, G. (2014) Restriction of gas losses in a overpressurised CO₂ reservoir using gel technology. *International journal of Oil , Gas and Coal Technology*, 8, 135–152.
- Manceau, J., Hatzignatiou, D.G., Lary, L. De, Jensen, N.B., and Réveillère, A. (2014) Mitigation and remediation technologies and practices in case of undesired migration of CO₂ from a geological storage unit — Current status. *International Journal of Greenhouse Gas Control*, 22, 272–290. Elsevier Ltd.
- Metin, C.O., Rankin, K.M., and Nguyen, Q.P. (2014) Phase behavior and rheological characterization of silica nanoparticle gel. 93–101.

- Provis, J.L., Duxson, P., Lukey, G.C., Separovic, F., Kriven, W.M., Deventer, J.S.J. van (2005) Modeling Speciation in Highly Concentrated Alkaline Silicate Solutions. *Ind. Eng. Chem. Res.* **44**, 8899-8908.
- Prud'homme, E. (2011) *Rôles du cation alcalin et des renforts minéraux et végétaux sur les mécanismes de formation de géopolymères poreux ou denses*. Ph.D. Univ. Limoges, 150 p.
- Stavland, A., Jonsbråten, H.C., Vikane, O., Skrettingland, K., and Fischer, H. (2011) In-Depth Water Diversion Using Sodium Silicate on Snorre - Factors Controlling In-Depth Placement. in: Proceeding of the Society of Petroleum Engineers SPE 143836.
- Tognonvi, M., Massiot, D., Lecomte, A., Rossignol, S., and Bonnet, J.P. (2010) Identification of solvated species present in concentrated and dilute sodium silicate solutions by combined ²⁹Si NMR and SAXS studies. *Journal of Colloid and Interface Science*, 352, 309–315.
- Tognonvi, M., Rosignol, S., and Bonnet, J.P. (2011a) Physical-chemistry of sodium silicate gelation in an alkaline medium. *Journal of Sol-Gel Science and Technology*, 58, 625–635.
- Tognonvi, M.T., Rossignol, S., and Bonnet, J. (2011b) Effect of alkali cation on irreversible gel formation in basic medium. *Journal of Non-Crystalline Solids*, 357, 43–49. Elsevier B.V.
- Tognonvi, M.T. (2009) *Physico-chimie de la gélification du silicate de sodium en milieu basique*. Ph.D Univ. Limoges, 166 p.
- Vail, J.G. (1952) *Soluble Silicates: their Properties and Uses*. Reinhold Publishing Corporation New York, 354 pp.

7 APPENDIX: BETOL K28 T SOLUTION

Table 8: Characteristics of the silicate solution provided by the manufacturer (Woellner).

Betol K28 T solution		Source
SiO ₂ content	20.5 wt% 2.645 mol/L	Manufacturer
SiO ₂ /K ₂ O	3.92	
K ₂ O	8.2 wt%	
pH	10.8 (*)	Manufacturer
	11.62	Measured
Specific density	1.25 g/cm ³	Manufacturer
Viscosity	28 mPa.s at 20°C	Manufacturer

(*) at a dilution of 10% in water

Table 9: Characteristics of the diluted solution

Betol K28 T / Water solution 50 : 50 by weight		Source
SiO ₂ content	1.90 mol/L	Manufacturer
pH	11.41	Measured
Specific density	1.11 g/cm ³ at 20°C	Measured
Viscosity	1.20 mPa.s at 29.7°C	Measured
	1.08 mPa.s at 41.9°C	
	0.99 mPa.s at 63.6°C	



Betol[®] K 28 T

Binder and Adhesive for Silicate based Coatings and Glues

Chemical description

Betol K 28 T is an inorganic binder based on an aqueous solution of potassium silicate.

Mode of action

Betol K 28 T reacts with and adheres to mineral surfaces by silicification. Due to the good bonding capacity and high temperature stability, fire and acid proof glues and sealants can easily be formulated.

Specification (average values)

Dry content:	approx. 28,0 %	007 *)
Density (20°C):	approx. 1,25 g/cm ³	042 *)
pH:	approx. 10,8	008 *)
(10 % in water)		
Viscosity (20°C):	approx. 28 mPas	053 *)
Solubility:	soluble in water in any proportion	

*) Internal method code – description available on request

Properties

- good bonding power and effect,
- excellent adhesion to mineral surfaces,
- heat and acid resistant,
- stable even under extreme climatic conditions,
- anticorrosive, antistatic, stable against UV radiation,
- alkaline liquid.

Application

- construction industry,
- construction chemicals,
- acid proof and refractories,
- mineral coatings,
- hardener for mineral (e.g. cement) based mortars or plasters,
- sealing of brick walls against rising humidity.

Note

Keep Betol K 28 T in closed receptacles. Before application a thorough hiding of glass, ceramics, light metals and natural stones is necessary. In case of spilling or splashing wash immediately with water. At the end of the work clean tools immediately with (warm) water.

Storage

Protect Betol K 28 T from frost. Storage stability in closed containers at least 12 months. Do not store Betol K 28 T in aluminium or galvanized receptacles.